

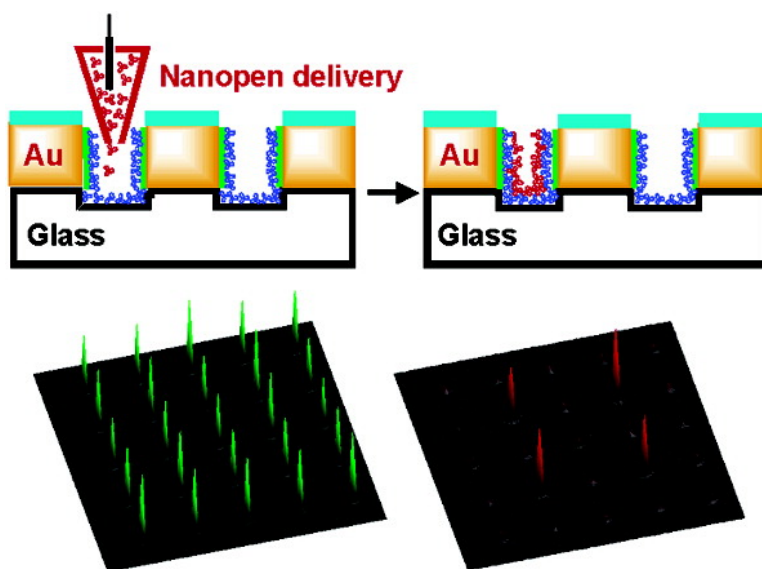
Communication

**An Addressable Antibody Nanoarray Produced on a Nanostructured Surface**

Andreas Bruckbauer, Dejian Zhou, Dae-Joon Kang, Yuri E. Korchev, Chris Abell, and David Klenerman

*J. Am. Chem. Soc.*, **2004**, 126 (21), 6508-6509 • DOI: 10.1021/ja0317426 • Publication Date (Web): 08 May 2004

Downloaded from <http://pubs.acs.org> on March 31, 2009



**More About This Article**

Additional resources and features associated with this article are available within the HTML version:

- Supporting Information
- Links to the 2 articles that cite this article, as of the time of this article download
- Access to high resolution figures
- Links to articles and content related to this article
- Copyright permission to reproduce figures and/or text from this article

[View the Full Text HTML](#)

## An Addressable Antibody Nanoarray Produced on a Nanostructured Surface

Andreas Bruckbauer,<sup>†</sup> Dejian Zhou,<sup>†</sup> Dae-Joon Kang,<sup>‡</sup> Yuri E. Korchev,<sup>§</sup> Chris Abell,<sup>†</sup> and David Klenerman<sup>\*†</sup>

*Department of Chemistry, University of Cambridge, Lensfield Road, Cambridge CB2 1EW, U.K., Nanoscience Center, IRC in Nanotechnology, University of Cambridge, 11 J J Thomson Avenue, Cambridge CB3 0FF, U.K., and Division of Medicine, Imperial College London, Hammersmith Hospital Campus, Du Cane Road, London W12 0NN, U.K.*

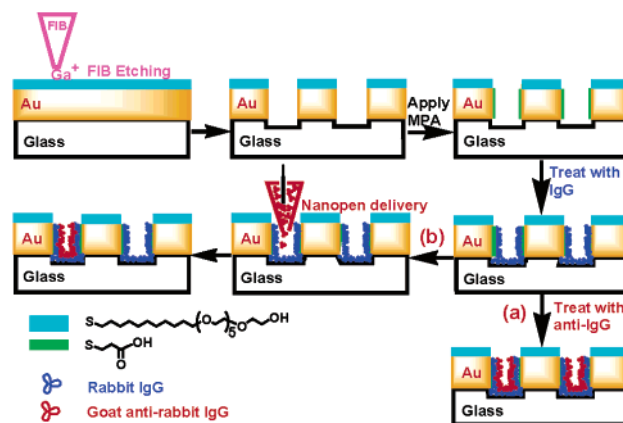
Received December 16, 2003; E-mail: dk10012@cam.ac.uk

There is a considerable interest in positioning functional biomolecules at defined positions on surfaces to produce biological arrays for analysis or to assemble complex and biologically functional structures using molecular recognition between different biomolecules.<sup>1</sup> The key issues are maintaining the functionality of the biomolecules, the smallest feature or spot size that can be obtained, the highest density of features possible, the ability to address a specific feature on the surface, and the ability to deposit different molecules to assemble complex structures.

One approach has been to use direct-write methods based on scanning probe microscopy (SPM).<sup>2–5</sup> Dip-pen nanolithography (DPN)<sup>2,3</sup> uses a functionalized AFM tip for delivery of molecules from the tip to the surface and operates in air. DPN has recently been used to deliver DNA and proteins.<sup>3</sup> We have developed a complementary method based on a nanopipet working in ionic solutions.<sup>4</sup> An ion current that flows between an electrode in the pipet and the bath is used to control the distance from the surface. The nanopipet acts as a nanopen, locally delivering biomolecules from the pipet tip, which then diffuse to the surface. The delivery is controlled by the sign and magnitude of the applied voltage, enabling control of the number of molecules delivered.<sup>4</sup> The biomolecules are always in buffered solution and maintain their biological activity. We have recently shown that we can deliver controlled numbers of functional biomolecules, including DNA and antibodies, to a surface, that the antibody–antigen interactions are specific, and that we can address a specific feature on the surface with a second biomolecule.<sup>4b</sup>

Work to date using SPM methods has been performed on flat surfaces, where the feature size is controlled by wetting or diffusion.<sup>2–5</sup> Here, we report the use of a novel nanofabricated surface, produced by a gallium ion focused ion beam microscope (FIB),<sup>6</sup> patterned with distinct chemical functionalities at defined positions. The structure has similarities to that used by Webb and co-workers for single molecule detection<sup>7</sup> and consists of regularly spaced holes. However, in this work, the holes were produced within a thin film (50 nm) of gold. This allows the position of a nanopipet, held in solution over the holes, to be observed through the gold by optical microscopy, enabling us to address individual holes. The bulk of the gold surface was coated with a self-assembled monolayer (SAM) terminated with hexa(ethylene glycol) (EG<sub>6</sub>) groups to resist nonspecific adsorption,<sup>8</sup> while the holes were functionalized with a SAM of 3-mercaptopropionic acid (MPA) to facilitate the immobilization of IgG antibodies (Scheme 1) mainly through electrostatic interactions.<sup>9</sup> Biomolecules in solution or delivered from the nanopipet thus adsorbed preferentially into the holes. Furthermore, the detection volume for fluorescence spectroscopy was confined to

**Scheme 1.** Schematic Showing the Procedure for the Fabrication, Modification, Solution Filling (Route a), and Nanopipet Addressing (Route b) with Antibodies of the FIB Nanofabricated Holes



the volume inside the hole because of the optical properties of the gold.<sup>7</sup> We show that we can fill these nanofabricated holes with proteins and that the feature size is determined by the size of the holes. Functional antibodies were delivered into specific holes to address them individually, and their binding was detected by confocal fluorescence microscopy.

Scheme 1 outlines the experimental procedures. We produced holes of two different sizes by FIB. The smaller holes were typically ellipsoidal possibly due to a beam drift during patterning. Measurements at the hole opening showed  $175 \pm 10$  nm for the major axis and  $150 \pm 10$  nm for the minor axis. The width of the holes decreased with depth; the full widths at half depth were  $85 \pm 7$  and  $50 \pm 6$  nm, respectively (Supporting Information, Figure S1). After the FIB patterning, the surface was incubated with a MPA solution for 1 h to coat the exposed gold with a MPA SAM. After that, the surface was incubated with a solution of Alexa 488 labeled IgG, washed to remove unbound IgGs, and then incubated with a solution of Alexa 647 labeled anti-IgG (Scheme 1, route a). Both green (from IgG) and red (from anti-IgG) fluorescence, detected simultaneously, were observed exclusively from the holes (Figure 1A). This demonstrates that these small holes can be filled with antibodies and is consistent with antibody–antigen interaction between the bound IgG and the anti-IgG from solution.

We then went on to address individual holes by delivering anti-IgG from the nanopipet. Because the outer diameter of the nanopipet is about 240 nm,<sup>4a</sup> larger holes (diameter:  $\sim 300$  nm at hole opening, depth  $\approx 90$  nm) were used so that the pipet could enter the hole (Supporting Information, Figure S2). The depth of these holes indicated that the FIB had milled into the glass layer. The holes were first filled with Alexa 488 labeled IgG from solution. After the sample was washed, the nanopipet was used to fill selected holes with Alexa 647 labeled anti-IgG (Scheme 1, route b). This

<sup>†</sup> Department of Chemistry, University of Cambridge.

<sup>‡</sup> Nanoscience Center, University of Cambridge.

<sup>§</sup> Imperial College London.

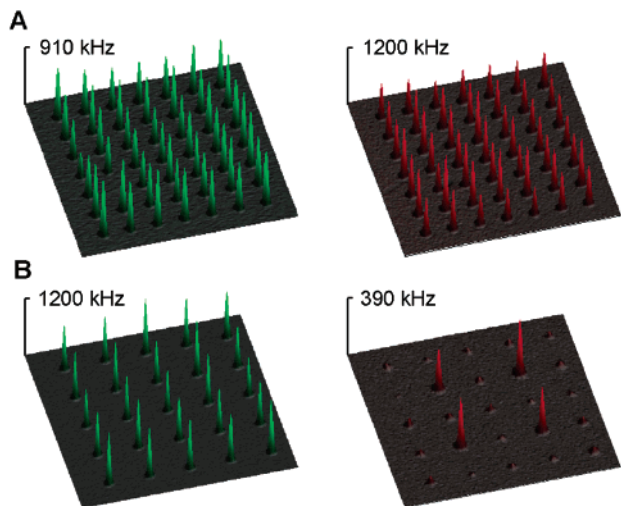


**Figure 1.** 3D representations of fluorescence images obtained from small holes, and bigger holes addressed by nanopipet delivery. The  $z$ -axis in the figure is the fluorescence count rate. (A) A surface nanostructured with  $7 \times 7$  holes (60–90 nm in diameter), after treatment with the solutions of IgG (labeled with Alexa 488) and then anti-IgG (labeled with Alexa 647) under blue (488 nm, left image) and red (632.8 nm, right image) laser excitations (image size:  $20 \mu\text{m} \times 20 \mu\text{m}$ ). (B) A surface nanostructured with  $5 \times 5$  holes (250–300 nm in diameter) after treatment with the IgG solution and then selective deposition of anti-IgG into 4 of the 25 holes using the nanopipet under blue (488 nm, left image) and red (632.8 nm, right image) laser excitations (size  $34 \mu\text{m} \times 34 \mu\text{m}$ ).

was accomplished by moving the pipet with ion-current distance control backward and forward ( $\pm 1.5 \mu\text{m}$ ) in a line over each selected hole for 30 s. The position of the hole could be identified by the dip in the simultaneously recorded topographic line scan. The green fluorescence (from IgG) was exclusively detected from the holes, and the intensity from each hole was similar (Figure 1B, left). The red fluorescence (from anti-IgG) clearly showed that specific holes, containing IgG, could be addressed with the secondary antibody by the nanopipet (Figure 1B, right). Combined fluorescence images of the two colors clearly indicated the IgG and anti-IgG were co-localized (Supporting Information, Figure S3).

A parallel experiment based on AFM images taken on small and shallow holes with sizes comparable to the small holes filled from solution ( $180 \pm 8$  nm in diameter at opening,  $16 \pm 1$  nm deep, Supporting Information, Figure S4), and larger holes with sizes comparable to those being addressed by the nanopipet ( $285 \pm 15$  nm in diameter,  $25 \pm 3$  nm deep, Supporting Information, Figure S5), produced within a flat template-stripped gold surface<sup>10</sup> under identical conditions, indicated that the antibodies preferably stuck to the side walls and the bottom of the holes. The apparent diameter and the depth of holes were reduced by  $\sim 20$  and 10 nm, respectively (Supporting Information, Figures S4 and S5). The AFM images also showed that some IgGs adsorbed around the edges of the larger holes, although this was about 100 times less than that in the holes. There was little evidence of nonspecific IgG adsorption in the case of the smaller and shallower holes, probably due to the use of a shorter milling time and smaller ion beam current leading to minimum damage of the PEG coating. Thus, in both cases, the adsorbed antibody feature size is determined by the hole size. For the small holes, this is 180 nm at the opening and 90 nm at the half depth.

The use of the nanofabricated surfaces has several advantages. First, it provides a region with different chemical functionality for selective adsorption of biomolecules to produce a nanoarray of biomolecules. The antibody feature size was determined by the nanofabricated hole and is comparable to those achieved by DPN<sup>3d,e</sup> or nanocontact printing.<sup>11</sup> Second, it provides a topographic feature

enabling one to return to the same position on the surface. Third, it defines the measurement region. The fluorescence from molecules outside the holes is blocked by the low transparency of the 50 nm thick gold layer, so there is a very low background in the fluorescence images (Figure 1), and the measurement is not affected by adsorption outside the hole.

In the addressing experiment, a small amount ( $\sim 10\%$ ) of the anti-IgG was also detected from holes that were not addressed by the nanopipet (Figure 1B). This is presumably due to some anti-IgGs delivered outside the holes diffusing over the surface and binding into neighboring holes during the pipet scanning. The delivery of molecules only when the nanopipet is in the hole, by using temporal control of the applied voltage, should reduce this cross contamination.

In summary, we have demonstrated that it is possible to selectively address specific features in a nanoarray by nanopipet delivery of a functional antibody. The addressed feature size,  $\sim 300$  nm in diameter, is a significant improvement over the spot size achieved by delivery with the nanopipet directly onto a flat surface (800 nm).<sup>4</sup> To our knowledge, this is the first example of addressing specific biologically functional features on a surface at the nanoscale.<sup>3</sup> This method could be extended to perform local assembly of biological structures or to perform a local assay by delivery of reagents from the pipet at defined positions on the surface.<sup>4a,b</sup> Direct writing on a nanofabricated surface should be a powerful combination for the performance of miniaturized analysis or creation of novel biological assemblies on the nanoscale.

**Acknowledgment.** We thank the BBSRC (U.K.) and the Cambridge IRC in Nanotechnology (U.K.) for funding this project.

**Supporting Information Available:** Details of the experimental procedures, AFM images of the nanostructured holes, and combined fluorescence images from small and big holes. This material is available free of charge via the Internet at <http://pubs.acs.org>.

## References

- (1) (a) Wilson, D. S.; Nock, S. *Angew. Chem., Int. Ed.* **2003**, *42*, 494. (b) MacBeath, G.; Schreiber, S. L. *Science* **2000**, *289*, 1760. (c) Seeman, N. C. *Nature* **2003**, *421*, 427. (d) Niemeyer, C. M. *Angew. Chem., Int. Ed.* **2001**, *40*, 4128. (e) Liu, F.; Sha, R.; Seeman, N. C. *J. Am. Chem. Soc.* **1999**, *121*, 917.
- (2) (a) Piner, R. D.; Zhu, J.; Xu, F.; Hong, S. H.; Mirkin, C. A. *Science* **1999**, *283*, 661. (b) Agarwal, G.; Sowards, L. A.; Naik, R. R.; Stone, M. O. *J. Am. Chem. Soc.* **2003**, *125*, 580.
- (3) (a) Wilson, D. L.; Martin, R.; Hong, S.; Cronin-Golomb, M.; Mirkin, C. A.; Kaplan, D. L. *Proc. Natl. Acad. Sci. U.S.A.* **2001**, *98*, 13660. (b) Agarwal, G.; Naik, R. R.; Stone, M. O. *J. Am. Chem. Soc.* **2003**, *125*, 7408. (c) Demers, L. M.; Ginger, D. S.; Park, S. J.; Li, Z.; Chung, S. W.; Mirkin, C. A. *Science* **2002**, *296*, 1836. (d) Lee, K. B.; Lim, J. H.; Mirkin, C. A. *J. Am. Chem. Soc.* **2003**, *125*, 5588. (e) Lim, J. H.; Ginger, D. S.; Lee, K. B.; Heo, J.; Nam, J. M.; Mirkin, C. A. *Angew. Chem., Int. Ed.* **2003**, *42*, 2309.
- (4) (a) Bruckbauer, A.; Ying, L. M.; Rothery, A. M.; Zhou, D. J.; Shevchuk, A. I.; Abell, C.; Korchev, Y. E.; Klenerman, D. *J. Am. Chem. Soc.* **2002**, *124*, 8810. (b) Bruckbauer, A.; Zhou, D. J.; Ying, L. M.; Korchev, Y. E.; Abell, C.; Klenerman, D. *J. Am. Chem. Soc.* **2003**, *125*, 9834. (c) Ying, L. M.; Bruckbauer, A.; Rothery, A. M.; Korchev, Y. E.; Klenerman, D. *Anal. Chem.* **2002**, *74*, 1380–1385.
- (5) Taha, H.; Marks, R. S.; Gheber, L. A.; Rousso, I.; Newman, J.; Sukenik, C.; Lewis, A. *Appl. Phys. Lett.* **2003**, *83*, 1041–1043.
- (6) Li, H. W.; Kang, D.-J.; Blamire, M. G.; Huck, W. T. S. *Nanotechnology* **2003**, *14*, 220–223.
- (7) Levene, M. J.; Korlach, J.; Turner, S. W.; Foquet, M.; Craighead, H. G.; Webb, W. W. *Science* **2003**, *299*, 682.
- (8) (a) Prime, K. L.; Whitesides, G. M. *Science* **1991**, *252*, 1164. (b) Zhou, D. J.; Bruckbauer, A.; Ying, L. M.; Abell, C.; Klenerman, D. *Nano Lett.* **2003**, *3*, 1517.
- (9) (a) Lee, K. B.; Park, S. J.; Mirkin, C. A.; Smith, J. C.; Mirksich, M. *Science* **2002**, *295*, 1702. (b) Zhou, D. J.; Wang, X. Z.; Birch, L.; Rayment, T.; Abell, C. *Langmuir* **2003**, *19*, 10557.
- (10) (a) Zhou, D. J.; Sinniah, K.; Abell, C.; Rayment, T. *Langmuir* **2002**, *18*, 8278. (b) Hegner, M.; Wagner, P.; Semenza, G. *Surf. Sci.* **1993**, *291*, 39.
- (11) (a) Renault, J. P.; Bernard, A.; Juncker, D.; Michel, B.; Bosshard, H. R.; Delamarche, E. *Angew. Chem., Int. Ed.* **2002**, *41*, 2320. (b) Li, H. W.; Muir, B. V. O.; Fichet, G.; Huck, W. T. S. *Langmuir* **2003**, *19*, 1963.

JA0317426